Effect of cholecalciferol on unsaturated model membranes**Title:** Effect of cholecalciferol on unsaturated model membranes

Authors: Aarthi Devarajan[1], Yeu-Chun Kim[2], A. F. Isakovic[3], Deborah L. Gater[4]*

Addresses: 1 Khalifa University, Abu Dhabi, UAE; 2 Korea Advanced Institute of Science and Technology (KAIST), Daejeon, Republic of Korea, 3 Colgate University, Hamilton, NY, USA, 4 University College London, London, UK

Corresponding author: Deborah L. Gater (email: d.gater@ucl.ac.uk and deborahlgater@gmail.com, corresponding address: Centre for Languages and International Education, University College London, 26 Bedford Way, London, WC1H 0AP, UK)

Author contributions: AD, AFI and DLG designed experiments, conducted experiments, analyzed data and contributed to manuscript preparation; YCK contributed to project development and discussion.

Competing Interests: The authors declare no competing interests

Figures: All figures (except the Graphical Abstract) are intended to be reproduced in black and white
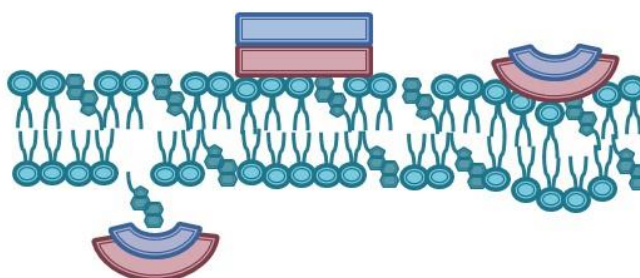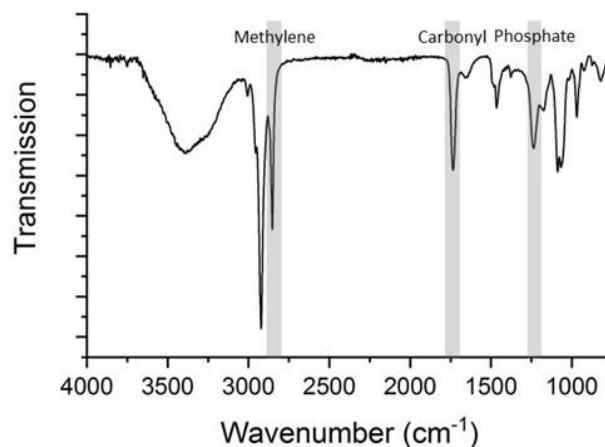
Abbreviations: **DBP** vitamin D binding protein, **DLS** dynamic light scattering, **DOPC** 1,2-dioleoyl-*sn*-glycero-3-phosphocholine, **LUV** large unilamellar vesicle, **MLV** multi-lamellar vesicle, **VitD** vitamin D,

Graphical Abstract:

Multilamellar vesicle Fourier-transform infrared spectrum →
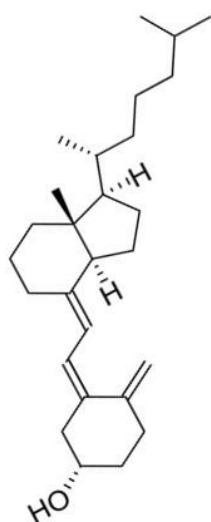
Vitamin D ↑   Cartoon of potential peripheral membrane-protein interactions ↑

Abstract:

Vitamin D plays an important role in many physiological processes, particularly calcium and phosphorous homeostasis. The biochemistry of vitamin D is also complex, encompassing a range of active molecules that may be either endogenous or dietary in origin. The role of lipids and fats in the production, processing and use of vitamin D is an interesting one, with a relative paucity of model studies into the interactions of vitamin D with lipidic systems such as micelles and vesicles. Here, we have studied the effect of vitamin D3 in simple unsaturated phospholipid systems. We used NMR and FTIR spectroscopy to investigate the effect of increasing vitamin D concentration on the structure and dynamics of the lipid chains and interfacial region. In order to link these model studies with more complex biomimetic environments, we compare results in the presence of buffer and vitamin D binding protein. We have also used DLS to determine that vitamin D3-DOPC vesicles can retain their size distribution for varying amounts of time in different conditions. We find that the acyl chain region of vitamin D3-DOPC membranes are generally disordered, and that the addition of buffer and/or protein alters the properties of the interfacial region.

Introduction:

Vitamin D (VitD) deficiency and insufficiency remain a public health concern around the world (1,2). In addition to the well-established role of VitD in rickets and musculoskeletal disorders (3-5), the association of VitD with a range of conditions, including certain cancers (6,7), diabetes (8,9), and cardiovascular disease (10) has been studied. However, many studies into the clinical consequences of the lack of VitD are inconclusive (11-14), and there is a great need for a more complete understanding of the complex biochemical and biophysical properties of this group of compounds (15,16). The development of improved formulations of vitamin D for delivery, including in oral administration, food fortification and for transdermal delivery (17-19), also remains a topic of interest.

VitD is hydrophobic and is derived from either the mammalian cholesterol precursor 7-dehydrocholesterol (producing VitD3), or from an ergosterol equivalent (producing VitD2). Endogenous VitD3 is produced by the action of UV light on 7-dehydrocholesterol in the plasma membrane of the epidermis (20). Dietary VitD (VitD2 or VitD3) is absorbed primarily via mixed micelles (21,22), although there is some indication that phospholipid vesicles may also be involved in this process. There are also reports of the involvement of active VitD metabolites in matrix vesicles involved in bone calcification (23). These biochemical factors make the study of VitD in phospholipid membranes relevant to several clinically significant questions.

Compared with many other sterols and sterol-derived membrane components, there is a relative paucity of research into the behavior of VitD in model membranes. In an effort to model the cutaneous production of VitD, HPLC has been used to quantify the degree of conversion from 7-dehydrocholesterol to VitD in liposomal systems, with more rapid conversion observed in more ordered membranes (24). On a similar theme, the differing effects of VitD3 (cholecalciferol) and ProVitD3 on 1,2-dipalmitoyl-*sn*-glycero-3-phosphocholine (DPPC) membranes were investigated calorimetrically, with VitD3 being more destabilizing to the membrane than its precursor (25). The different effects of cholesterol and VitD3 on the thermotropic phase behavior of model membranes containing saturated lipids of various chain lengths has also been studied (26). VitD3 behaved differently to cholesterol in a number of ways; for example, the lipid acyl chains were more sensitive to VitD3 as chain length increased, whereas sensitivity to cholesterol decreased with chain length. A more exhaustive x-ray study of VitD3 and VitD2 (ergocalciferol) in DPPC membranes focused on the effects of increasing concentrations of the vitamins in decreasing the gel to fluid phase transition temperature, and in modulating the structure of the gel phase (27). A study of the VitD2-DPPC system used FTIR to examine the localization of VitD2 in DPPC membranes (28), concluding that VitD2 resided primarily in the hydrophobic center of the bilayer, with evidence for proximity of the VitD2 hydroxyl groups to the lipid carbonyl groups. Other studies of VitD2 have produced observations regarding the competing effects of calcium phosphate (29) or Mg^{2+} ions (30) on VitD2-containing DPPC liposomes, using FTIR and calorimetry, and have investigated the properties of liposomes encapsulating vitamin D and curcumin (31). There has been considerable work on emulsification and nano-structured lipid carriers for food fortification with vitamin D (for example, those described here (19)), but these generally fall outside the scope of the current work.

The present work offers novel insights into the behavior of VitD3 in an unsaturated model membrane comprising 1,2-dioleoyl-*sn*-glycero-3-phosphocholine (DOPC, see Figure 1), and into the effects of the buffer and the physiologically important vitamin D binding protein. FTIR and NMR

spectroscopies were used to probe the membrane at the functional group level, focusing on phosphate, carbonyl and methylene to examine both interfacial and hydrophobic regions of the bilayers.
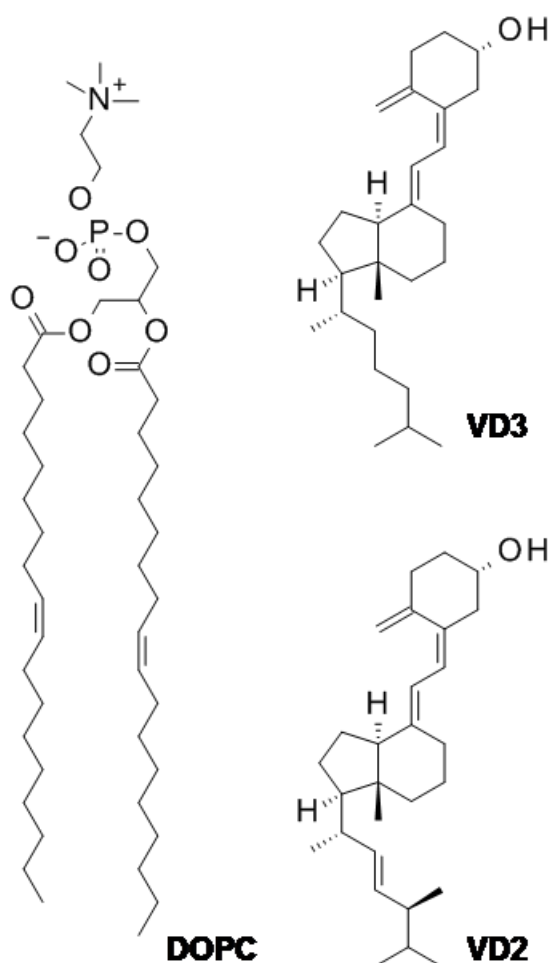

Figure 1: Molecular structures of 1,2-dioleoyl-*sn*-glycero-3-phosphocholine (DOPC), vitamin D3 (VD3, cholecalciferol) and vitamin D2 (VD2, ergocalciferol).

Material and Methods:

Materials: 1,2-dioleoyl-*sn*-glycero-3-phosphocholine (DOPC) was bought from Avanti Polar Lipids (Alabama, US). Cholecalciferol (Vitamin D3, VitD3) 98% HPLC purified and D_2O were purchased from Sigma Lifesciences. Deionized water was used as solvent for all sample preparation unless otherwise specified. Phosphate buffered saline (PBS tablets producing a solution of 0.01M phosphate buffer, 0.0027M potassium chloride and 0.137M sodium chloride at pH 7.4) was obtained from Sigma Aldrich (US). Vitamin D binding protein, Globulin GC was bought from Athens Research (Georgia, US). All materials were used without further purification.

Sample Preparation: Multilamellar Vesicles (MLV) with DOPC-VitD3 complex were formulated at desired mole percent ratios (15:85, 20:80, 25:75, and 30:70 of VitD3: DOPC respectively). MLVs were prepared by thin film hydration method where the blend of DOPC and VitD3 were first dissolved in chloroform and the solvent was removed using a dry nitrogen stream and the samples were kept in vacuum for overnight. The resulting thin film was then hydrated in an aqueous phase. The hydrated

samples were flash frozen using liquid nitrogen and lyophilized overnight. Dry samples were stored at -20°C until needed, and then hydrated by the addition of 66wt% H_2O, D_2O or buffer as indicated for characterization by FTIR or NMR and/or LUV preparation.

Large Unilamellar Vesicles (LUV) were prepared by extrusion, where MLVs were hydrated in distilled water, D_2O or buffer and extruded 15 times through 0.1 µm polycarbonate filters with a Mini-Extruder (Avanti Polar Lipids). LUVs were further utilized for stability studies using dynamic light scattering.

Protein Studies: Vitamin D binding protein (Globulin GC) was reconstituted in 366 µl of deionized water for a final protein concentration of 3.76 mg/ml. Buffer samples were prepared with PBS pellets dissolved in deionized water. 3 µl of either protein or buffer samples were mixed with 25 µl of hydrated MLVs for further characterization. These concentrations give approximate vitamin-to-protein ratios of between 1600 and 3500 to 1, and phospholipid-to-protein ratios of between 9900 and 8100 to 1.

Fourier Transform Infrared (FTIR) Spectroscopy: Infrared spectra were measured at 25°C on a Fourier Transform Spectrophotometer (Spectrum 100 FT-IR Spectrometer, Perkin Elmer) with an MIR-TGS (mid-infrared TriGlycine Sulphate) detector and a Universal ATR accessory. Spectra were collected with the Perkin Elmer Spectrum Software at a scanning range 700-4000 cm^{-1}, scan speed of 0.20 cm/S with a resolution at 1 cm^{-1}. Approximately, 3 µl of sample was placed on the sample window and incubated for 10 mins before obtaining the spectra. An ATR correction factor of 0 was applied. Processing of the spectra included baseline correction and fitting the spectra using QuickPeaks in Origin Pro 2015 and 2018 (Origin LabCorp, US) to determine the peak center positions and widths (full width at half maximum). Carbonyl bands were also separately fit with up to two Gaussian peaks using the same software. Briefly, baseline correction was endpoint weighted, and positive peaks (maximum 2) were found via second derivatives with automatic smoothing. Starting parameters were identified by the fitting software and there were no constraints on position or width of the fits. More details on the parameters and outcome of these fits are provided in the Supplementary Material, Table S1.

Nuclear Magnetic Resonance (NMR) Spectroscopy: All NMR data were acquired on a 600MHz, narrow bore, Bruker (Karlsruhe, Germany) DRX spectrometer operating at 14.09T with a ^{1}H resonance of 600.1MHz, and a ^{13}C resonance of 150.9MHz. ^{13}C NMR MAS spectra were recorded in a 4mm two-channel cross polarization-MAS probe with spinning frequencies of 5kHz, using a standard cross-polarization pulse program with spinal64 ^{1}H decoupling at 50W. The ^{1}H 90° pulse was 4.5µs at 150W, and cross polarization was achieved with a contact time of 2000µs at a ^{1}H power of 150W and a ^{13}C power of 60W. A recycle delay of 2.0s was used and 4096 scans were acquired for all spectra. All data were analyzed using Bruker Topspin software v3.5 (Karlsruhe, Germany).

Dynamic Light Scattering (DLS): The hydrodynamic diameter (D_H), size distribution and the polydispersity index were determined by DLS measurements at 25°C on a Zetasizer Nano ZSP, Malvern Instruments, equipped with 10mW HeNe laser (wavelength λ=633 nm). The Nano ZSP incorporates non-invasive back scattering detection angle of 173° and using automatically adjusted laser attenuation filters. Samples were diluted in distilled water as dispersant and for the analysis, viscosity of 0.8872 mPa and refractive index of 1.33 were used in respect for the dispersant.

LUVs with lipid-VitD3 complex was made by dissolving 10 mg of the complex in 200 µl of distilled water and incubated for 1 hour at room temperature prior to extruding. The extruded samples are then diluted in distilled water (1:10 dilution). Stability studies were carried out at a time intervals of day 0, 1, 7 and 14 under storage conditions (in the presence and absence of light). Hydrodynamic

diameter (DH) and PDI results were given as mean of three repeated measurements with 12 runs of 10 S each.

Results and Discussion:

The effect of adding cholecalciferol (VitD3) to multilamellar vesicles (MLV) of 1,2-dioleoyl-*sn*-glycero-3-phosphocholine (DOPC) in water at room temperature was investigated by FTIR and NMR spectroscopies.

The FTIR data allowed analysis of the effects of these parameters on the methylene symmetric stretches, carbonyl stretch and asymmetric phosphate stretch bands (see Figure 2 for representative spectrum). Compared with the DOPC-only MLVs (labeled 0mol% VitD3 in Figure 3), addition of 15, 20, 25 or 30mol% VitD3 resulted in no significant change in the measured frequencies (2853-2854cm^{-1}) or peak widths (full-width half maximum – FWHM – 39-42cm^{-1}) of the methylene symmetric stretches in FTIR spectra. Changes in the frequency of methylene stretches in lipid systems have previously been correlated with changes in the proportion of gauche conformations in the lipid chain – i.e. increasing frequency corresponds to an increase in chain disorder (32-34), although this effect is predominantly reported in saturated-chain lipids. The frequency of the methylene symmetric stretch in the DOPC-VitD3 is at the higher end of the range reported by Mendelsohn et al (2848-2854cm^{-1}, see Table 1 in reference (32)), indicating the generally high degree of chain disorder in this system – expected for the unsaturated DOPC acyl chain. The FTIR results are confirmed by NMR data for samples containing VitD3 (Figure 4), as there is minimal change in the chemical shift of the bulk methylene peak (from 29.74 to 29.65ppm) between 15 and 30mol% VitD3 (35-37). As both DOPC and VitD3 contain straight chain (non-ring) methylene groups (32 moieties in DOPC, and 3 in VitD3 – see Figure 1), there is expected to be some contribution from both molecules in this peak. However, DOPC provides the dominant contribution – even at 30mol% VitD3, only 4% of methylene groups in the system are from VitD3 (calculated based on structures in Figure 1).
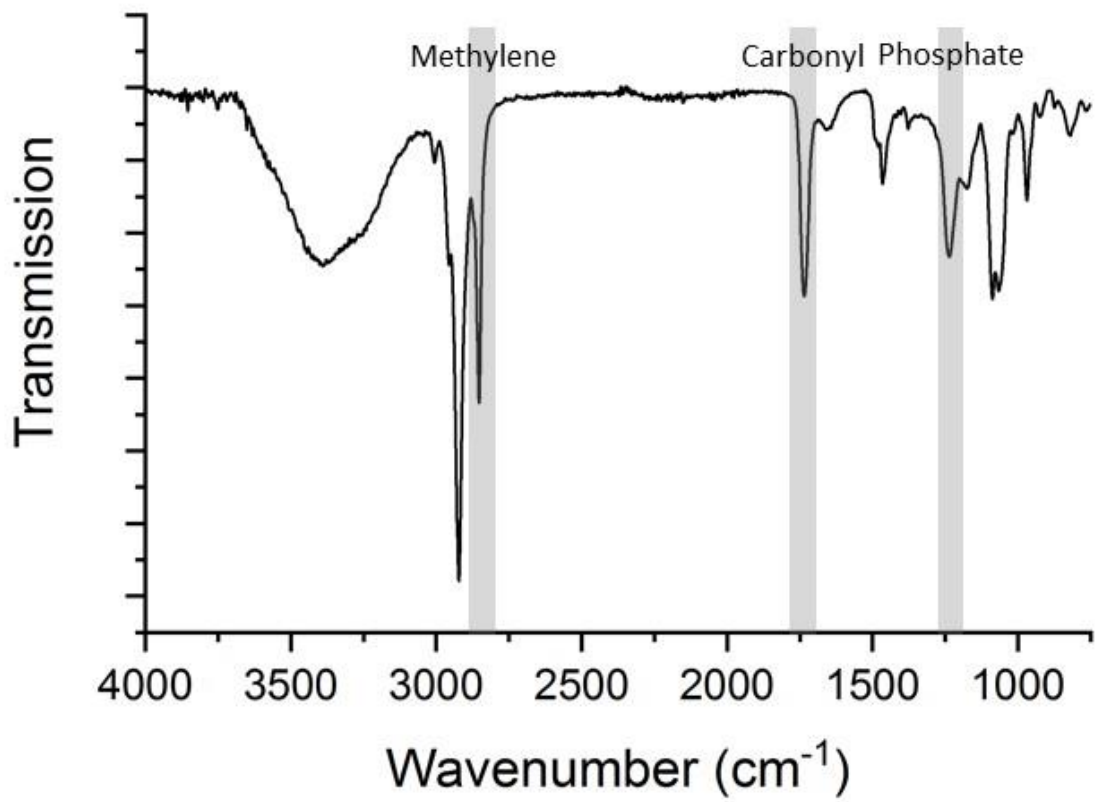
Figure 2. Representative room temperature FTIR spectrum of DOPC multilamellar vesicles in distilled water.
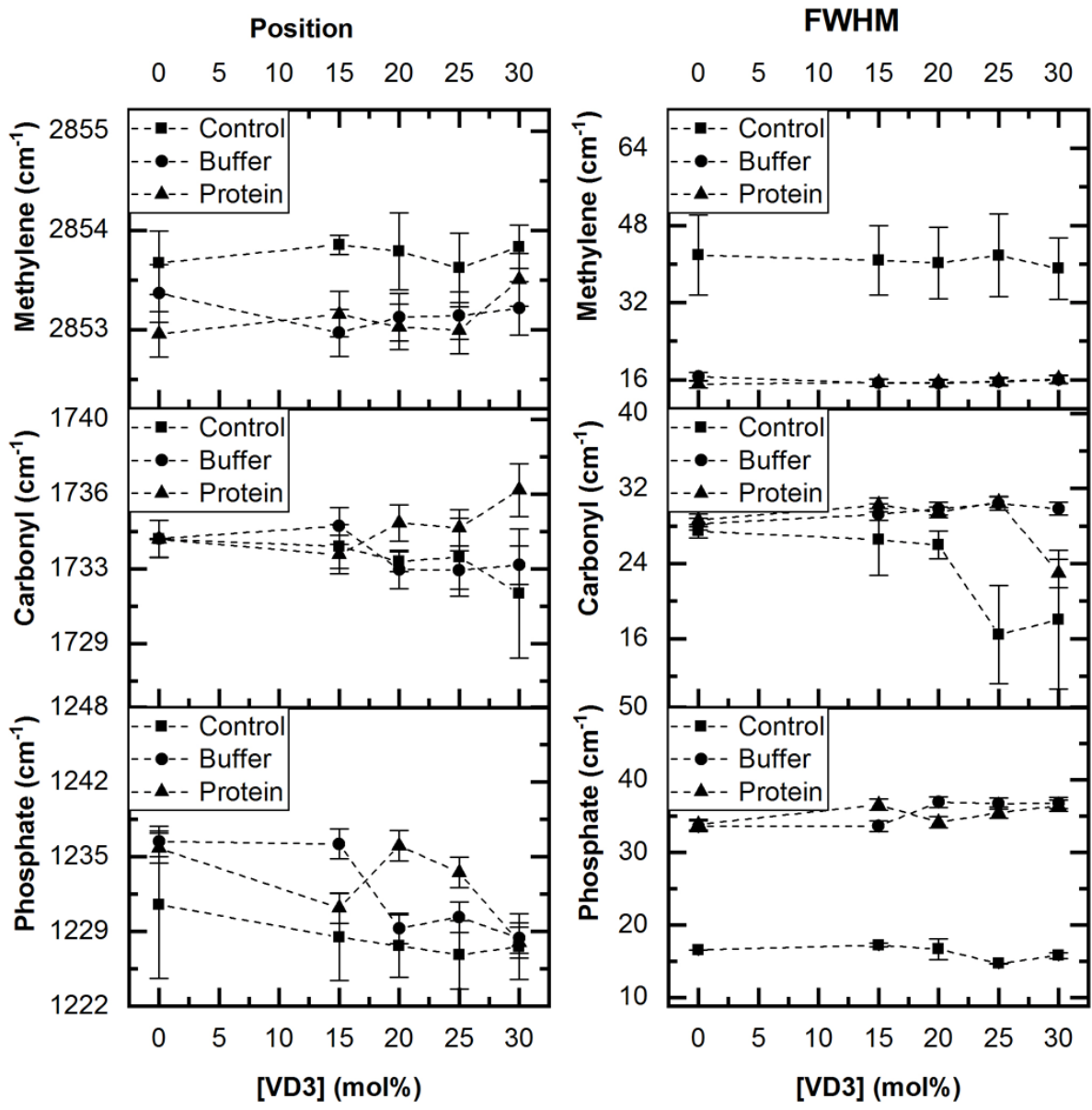
Figure 3: Room temperature FTIR data for multilamellar vesicles containing DOPC with the specified amount of vitamin D3 (VD3) in distilled water (water), phosphate buffered saline solution (buffer) or in buffer with vitamin D binding protein (protein). Left panel shows changes in band frequency for methylene symmetric stretch, carbonyl stretch and phosphate asymmetric stretch. Right panel shows changes in FWHM for the same bands.
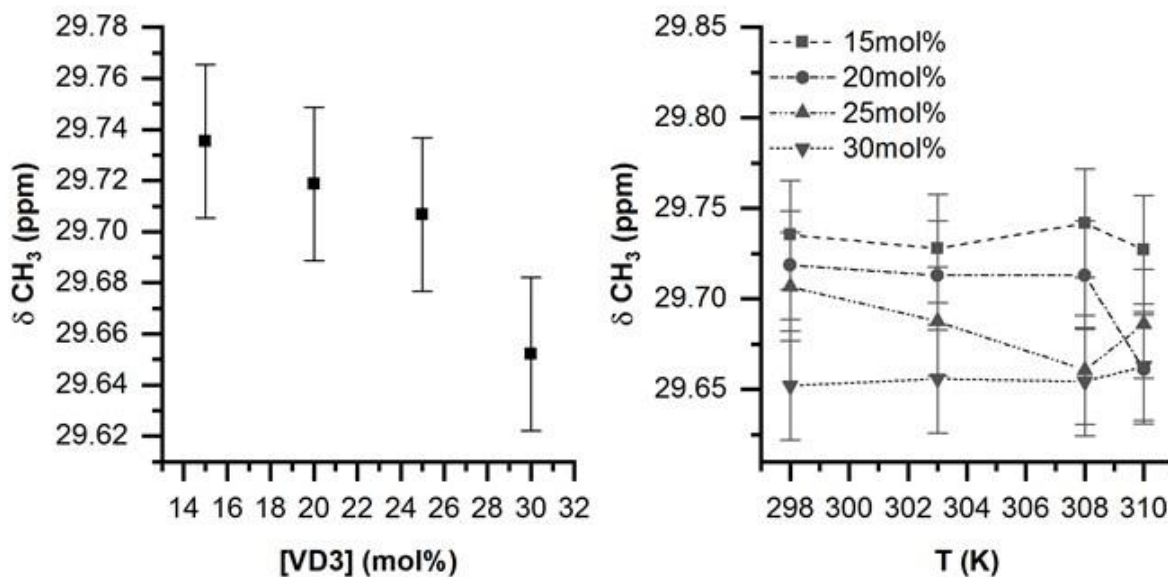
Figure 4: (Left) ^{13}C-NMR chemical shift (δ CH$_3$) data for the DOPC bulk acyl chain methylene peak as a function of vitamin D3 content. Data were acquired in multilamellar vesicles at 298K. (Right) ^{13}C-NMR chemical shift (δ CH$_3$) data for the DOPC bulk acyl chain methylene peak as a function temperature at various vitamin D3 content (15mol% to 30mol% as indicated). Data were acquired in multilamellar vesicles.

The FTIR spectra also provide information regarding carbonyl and phosphate groups, at 1735-1725 and 1230-1220cm^{-1}, respectively (Figure 3). As the VitD3 molecule contains no carbonyl or phosphate groups, these bands can be unambiguously assigned to DOPC. The center of the carbonyl stretching peak decreases slightly from 1734 to 1731cm^{-1} between 0 and 30mol% VitD3. In other phospholipid systems, similar shifts have been attributed to changes in the proportion of carbonyl groups that are hydrogen-bonded (to water or other local hydrogen-bond donors, such as the alcohol group on VitD3 in this case), as the carbonyl band contains contributions from the two closely adjacent hydrogen-bonded and non-hydrogen-bonded peaks (38). The FWHM of the carbonyl peaks also decreases at 25 and 30mol% cholesterol – from 26-27cm^{-1} at lower concentrations of VitD3 to 16-18cm^{-1} at the two highest concentrations, indicating an increase in the homogeneity of the interfacial region with larger amounts of VitD3.

We have fitted the carbonyl stretching bands to a two-peak Gaussian model to determine how the proportion of hydrogen-bonded carbonyl groups alters according to the amount of VitD3 present (see Figure 5). Without constraining peak positions, we were able to resolve the two peaks seen in other studies – one centered around 1744cm^{-1} ($\pm$ 1.2 cm^{-1} standard deviation) and one centered around 1731cm^{-1} ($\pm$ 1.8 cm^{-1} standard deviation). We did also see variations in the relative areas of the underlying peaks. Interestingly, the change in relative areas of the underlying peak did not reflect the change in the overall band frequency – as the overall band frequency decreased slightly with increasing VitD3, we also observed a slight decrease in the contribution from the lower-frequency Gaussian associated with hydrogen-bonding (38) to the carbonyl group from 89% hydrogen-bonded to 51% hydrogen-bonded. The presence of the VitD3 hydroxyl group near the lipid-water interface presumably interferes with the DOPC-water hydrogen bonding, either by altering lipid interfacial spacing or by competing with the carbonyl for hydrogen-bonds to the water molecules in the interfacial region.
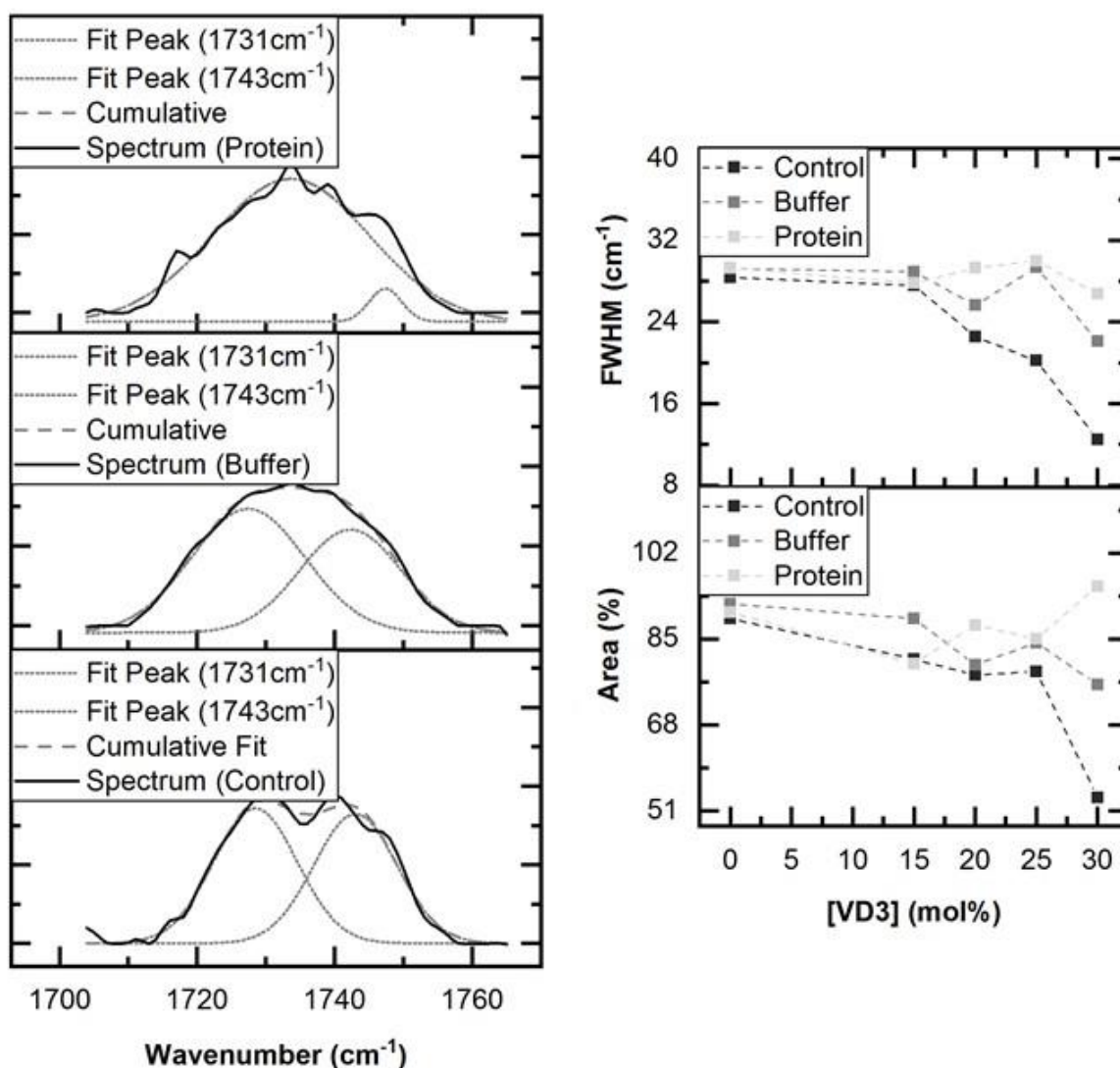
Figure 5: Results of fitting FTIR carbonyl bands. Left panel gives three examples of fit results for samples containing 30 mol% vitamin D3 (VD3) showing two fitted peaks with the cumulative fit overlaid on the spectrum. Right panel shows the effect of VD3 content on the area percent (proportion) of the peak centered around 1731 cm^{-1} (representative of hydrogen-bonded carbonyl) and the full width half maximum of the same fitted peaks.

The asymmetric phosphate stretch in the 0mol% VitD3 sample was centered at 1231cm^{-1}, whereas peaks for VitD3-containing samples were slightly lower in frequency (1226-1228cm^{-1}), with no strong concentration-dependent trend given the peak finding uncertainty (Figure 3). The value of ~1231cm^{-1} for the phosphate stretch in DOPC is similar to values previously reported for phosphatidylcholines (39,40), and in the same range as values previously reported for DOPC, albeit with the previous values being reported at lower hydration (5-20wt%, compared with 66wt% water in this study) (41). The FWHM of the phosphate peaks was the narrowest of the three types of peak discussed here, ranging from 15-17cm^{-1}, and showed no significant change with the changing VitD3 concentration.

All of the FTIR data reported in this work was acquired at room temperature due to the lack of a temperature control unit with the available instrumentation. Therefore, we used NMR spectroscopy to additionally investigate whether there was any significant difference in lipid acyl chain behavior at physiological temperature compared with room temperature (Figure 4). Neither the chemical shift nor the width (FWHM) of the peaks altered significantly between 25°C and 37°C, indicating that there was no substantial change in chain order or dynamics over this temperature range.

Once the effects of VitD3 on the DOPC lamellar phase at room temperature had been established, we used FTIR spectroscopy again to investigate the effects of adding small quantities of buffer (as a control to record ion concentration effects) or buffer with vitamin D binding protein (DBP). The results of this study are shown in Figure 3. In the case of the methylene symmetric stretch: the frequencies of the peaks in the control (water-only) samples were consistently slightly higher (~2854cm^{-1}) compared with the frequencies of the peaks in the buffer and protein samples (2853cm^{-1}), although the difference in frequency is small and at the limit of resolution. There was no substantial difference between buffer and protein samples, and again no effect of VitD3 concentration on the frequency of the methylene peak. However, in terms of FWHM, the width of the methylene peak in the buffer and protein samples was substantially less (15-17cm^{-1}) than the width in the water-only sample (39-42cm^{-1}). There was similarly no substantial difference between protein and buffer samples, and no effect of VitD3 concentration. These results indicate that there is a general increase in the homogeneity of the DOPC and DOPC-VitD3 membranes in the presence of buffer, and that this is likely an effect of ion concentration, irrespective of VitD3 or protein composition.

In the case of the carbonyl stretch, there was some distinction between protein and non-protein containing samples at higher VitD3 concentrations. In general, the carbonyl stretching frequency in the presence of protein increased with increasing VitD3 concentration (from 1734 to 1736cm^{-1}), whereas the frequency decreased with increasing VitD3 concentration in both water-only and buffer samples (from 1734 to 1731 and 1733cm^{-1}, respectively). When the carbonyl peaks were again fit to examine underlying hydrogen bonding (Figure 5), it became apparent that whereas the proportion of hydrogen-bonded carbonyl reduced as VitD3 increased in the control sample, this effect was less significant in the buffer sample and almost non-existent in the sample containing protein. The FWHM of the carbonyl peak was more sensitive to changing VitD3 concentration in the water-only sample than either the buffer or the protein samples. It is important to note that as protein was added at relatively small concentrations after the MLVs had been constituted, only a relatively small proportion of the lipid content may have been in contact with the protein. In order to further assess the effect of protein, it would be interesting either to add the protein during the reconstitution of the MLVs (to enable further penetration of the lipid layers), or to increase the concentration of protein, or both.

Results for the phosphate asymmetric stretching peak were much more consistent for the FWHM than for the peak frequency. That is, buffer and protein samples had consistently larger FWHM (34-37cm^{-1}) than the water-only sample (15-17cm^{-1}), with no substantial difference between protein and buffer samples, and a very slight trend to increase FWHM in protein and buffer samples as VitD3 concentration increased. This indicates that, in contrast to the methylene chains, where narrower peaks were observed, the phosphate head groups experience a less homogeneous environment in the presence of buffer and protein, which is somewhat unsurprising given the more complex composition.

The frequency of the phosphate stretch was consistently higher in protein and buffer samples than in water-only samples, except at 30% VitD3, when all three samples had a similar frequency (1227-1228cm^{-1}). At 0% VitD3, the frequency of the phosphate stretch was similar for buffer and

protein samples (1236cm^{-1}), and higher than that for the water only sample (1231cm^{-1}). Between these two concentrations, there was substantial variation in the frequencies of the peaks in the buffer and protein samples. The frequencies in the buffer samples decreased consistently from 1236cm^{-1} at 0 and 15% VitD3 to 1229-1230cm^{-1} at 20 and 25% VitD3, and then 1228cm^{-1} at 30% VitD3. In comparison, in the protein sample, the frequency decreased from 1236 to 1231cm^{-1} between 0 and 15% VitD3, and then increased again to 1236-1234cm^{-1} at 20 and 25% VitD3, before dropping to 1228cm^{-1} at 30% VitD3. The position of the phosphate band is known to be highly sensitive to hydration (39,40). Previously, a decrease of 15cm^{-1} was observed when increasing water composition from 5 to 20 wt% (41). The presence of various ions has also been shown to affect the phosphate band (42-44). Here, in samples of 66wt% hydration, with different ion contents, we see variation of less than 10 cm^{-1} with a general trend to increasing hydration at increasing VitD3 concentrations.

Finally, we used DLS to investigate whether VitD3 had any effect on the physical stability of DOPC liposomes over time. Liposomes were prepared via extrusion, using the same protocol for all samples, and were stored at room temperature for two weeks either in ambient light or in the dark. Immediately following extrusion, all samples showed a broad but monodisperse population of liposomes, with a diameter centered around 200nm for DOPC, 15mol% and 25mol% VitD3 (Figure 6). Samples containing 20mol% and 30mol% VitD3 were centered at ~250nm and had a slightly broader initial distribution of liposome sizes. DLS results were recorded again on days 1, 7 and 14. In general, the DOPC and 15mol% VitD3 samples retained their initial size distribution over the 2-week period, regardless of storage conditions. All samples with larger VitD3 contents showed some evidence of polydispersity, beginning on day 1 for the 30mol% VitD3 sample. The 20 and 25mol% VitD3 samples both exhibited polydispersity on day 7 when stored in the light, and the 20mol% sample also exhibited polydispersity on day 14 when stored in the dark.
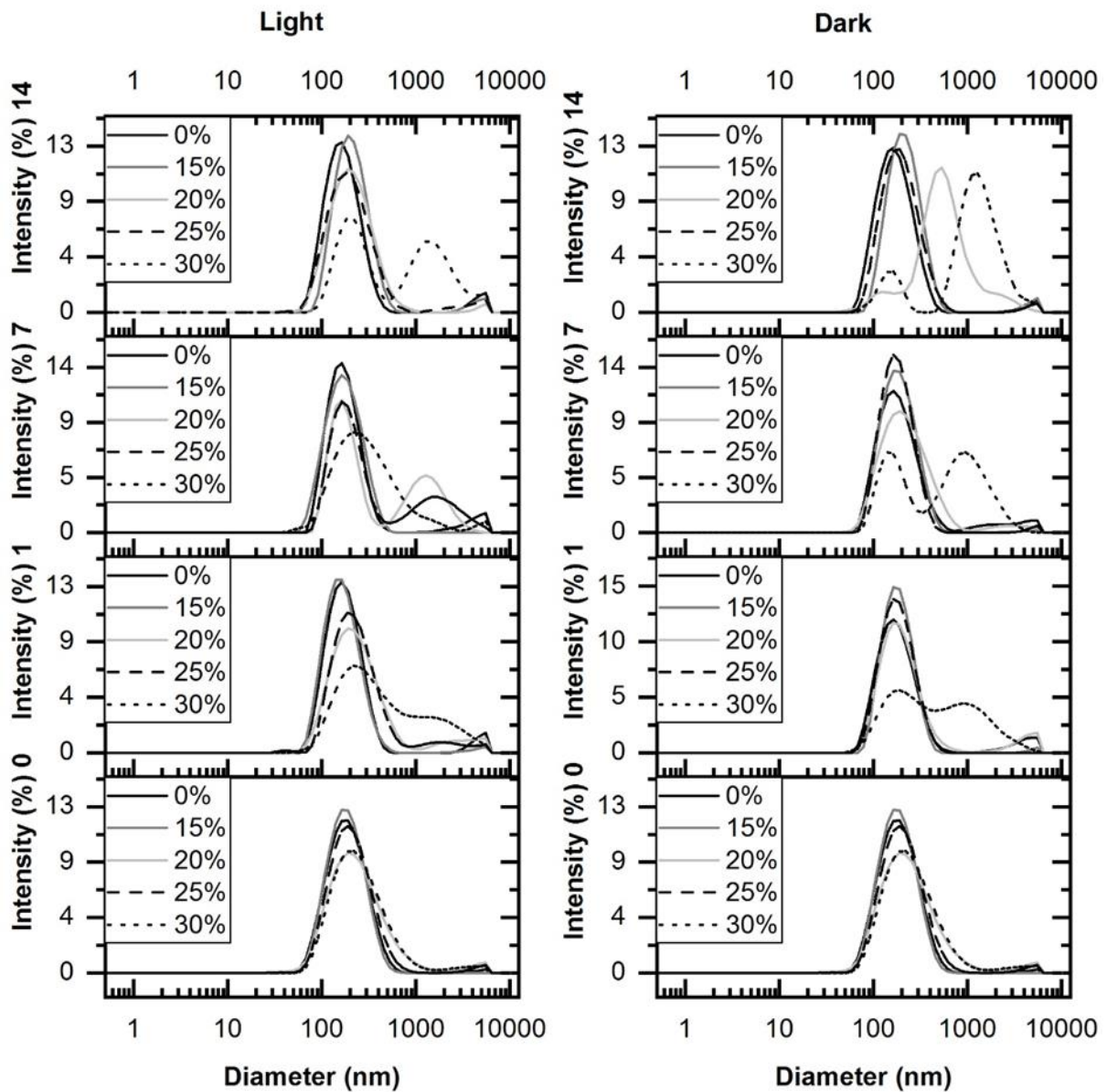
Figure 6: Dynamic light scattering data for large unilamellar vesicles comprising DOPC with 0%, 15%, 20%, 25% or 30% vitamin D3 as indicated in legend for each plot, stored at room temperature either in ambient light (left panel) or in the dark (right panel). Numbers on the y axes indicate days since sample preparation.

Conclusion:

In conclusion, the addition of up to 30mol% VitD3 has little effect on the proportion of gauche states or overall homogeneity of the already disordered DOPC acyl chains, but does slightly alter the interfacial and headgroup region of the membrane by reducing hydrogen-bonding at the carbonyl and increasing hydration at the phosphate. The addition of buffer increases the homogeneity of the DOPC acyl chains without altering overall structure, and similarly decreases the homogeneity of the phosphate environment.

These data suggest that the DOPC-VitD3 system may be useful for the further study of VitD3 in model membranes, including for studies of protein-vitamin and protein-lipid interactions, as the system is relatively robust across a range of temperatures and VitD3 concentrations, and LUVs with lower VitD3 concentrations also retain their size distribution for a substantial period of time.

References:

1. Holick, M. F. (2017) The vitamin D deficiency pandemic: Approaches for diagnosis, treatment and prevention. *Reviews in endocrine & metabolic disorders* **18**, 153-165
2. Mendes, M. M., Charlton, K., Thakur, S., Ribeiro, H., and Lanham-New, S. A. (2020) Future perspectives in addressing the global issue of vitamin D deficiency. *Proceedings of the Nutrition Society* **79**, 246-251
3. Wintermeyer, E., Ihle, C., Ehnert, S., Stockle, U., Ochs, G., de Zwart, P., Flesch, I., Bahrs, C., and Nussler, A. K. (2016) Crucial Role of Vitamin D in the Musculoskeletal System. *Nutrients* **8**
4. Levine, M. A. (2020) Diagnosis and Management of Vitamin D Dependent Rickets. *Frontiers in Pediatrics* **8**
5. Bhattarai, H. K., Shrestha, S., Rokka, K., and Shakya, R. (2020) Vitamin D, Calcium, Parathyroid Hormone, and Sex Steroids in Bone Health and Effects of Aging. *Journal of Osteoporosis* **2020**
6. Mondul, A. M., Weinstein, S. J., Moy, K. A., Mannisto, S., and Albanes, D. (2014) Vitamin D-binding protein, circulating vitamin D and risk of renal cell carcinoma. *International Journal of Cancer* **134**, 2699-2706
7. Holick, M. F. (2005) Vitamin D: Important for prevention of osteoporosis, cardiovascular heart disease, type 1 diabetes, autoimmune diseases, and some cancers. *Southern Medical Journal* **98**, 1024-1027
8. Harinarayan, C. V. (2014) Vitamin D and diabetes mellitus. *Hormones (Athens, Greece)* **13**, 163-181
9. Sung, C.-C., Liao, M.-T., Lu, K.-C., and Wu, C.-C. (2012) Role of Vitamin D in Insulin Resistance. *Journal of Biomedicine and Biotechnology*
10. Wang, T. J., Pencina, M. J., Booth, S. L., Jacques, P. F., Ingelsson, E., Lanier, K., Benjamin, E. J., D'Agostino, R. B., Wolf, M., and Vasan, R. S. (2008) Vitamin D deficiency and risk of cardiovascular disease. *Circulation* **117**, 503-511
11. Theodoratou, E., Tzoulaki, I., Zgaga, L., and Ioannidis, J. P. (2014) Vitamin D and multiple health outcomes: umbrella review of systematic reviews and meta-analyses of observational studies and randomised trials. *BMJ (Clinical research ed.)* **348**, g2035

12.   Pludowski, P., Holick, M. F., Pilz, S., Wagner, C. L., Hollis, B. W., Grant, W. B., Shoenfeld, Y., Lerchbaum, E., Llewellyn, D. J., Kienreich, K., and Soni, M. (2013) Vitamin D effects on musculoskeletal health, immunity, autoimmunity, cardiovascular disease, cancer, fertility, pregnancy, dementia and mortality-A review of recent evidence. *Autoimmunity Reviews* **12**, 976-989

13.   Akutsu, T., Kitamura, H., Himeiwa, S., Kitada, S., Akasu, T., and Urashima, M. (2020) Vitamin D and Cancer Survival: Does Vitamin D Supplementation Improve the Survival of Patients with Cancer? *Current Oncology Reports* **22**

14.   Faghfouri, A. H., Faghfuri, E., Maleki, V., Payahoo, L., Balmoral, A., and Bishak, Y. K. (2020) A comprehensive insight into the potential roles of VDR gene polymorphism in obesity: a systematic review. *Archives of Physiology and Biochemistry*

15.   Brannon, P. M., Yetley, E. A., Bailey, R. L., and Picciano, M. F. (2008) Summary of roundtable discussion on vitamin D research needs. *The American journal of clinical nutrition* **88**, 587s-592s

16.   Brannon, P. M. (2012) Key questions in Vitamin D research. *Scandinavian Journal of Clinical and Laboratory Investigation* **72**, 154-162

17.   Rejinold, N. S., Kim, H. K., Isakovic, A. F., Gater, D. L., and Kim, Y. C. (2019) Therapeutic vitamin delivery: Chemical and physical methods with future directions. *Journal of Controlled Release* **298**, 83-98

18.   Glowka, E., Stasiak, J., and Lulek, J. (2019) Drug Delivery Systems for Vitamin D Supplementation and Therapy. *Pharmaceutics* **11**

19.   Maurya, V. K., Bashir, K., and Aggarwal, M. (2020) Vitamin D microencapsulation and fortification: Trends and technologies. *J. Steroid Biochem. Mol. Biol.* **196**

20.   Tian, X. Q., Chen, T. C., Matsuoka, L. Y., Wortsman, J., and Holick, M. F. (1993) Kinetic and thermodynamic studies of the conversion of previtamin D3 to vitamin D3 in human skin. *J Biol Chem* **268**, 14888-14892

21.   Goncalves, A., Gleize, B., Roi, S., Nowicki, M., Dhaussy, A., Huertas, A., Amiot, M.-J., and Reboul, E. (2013) Fatty acids affect micellar properties and modulate vitamin D uptake and basolateral efflux in Caco-2 cells. *Journal of Nutritional Biochemistry* **24**, 1751-1757

22.   Reboul, E. (2015) Intestinal absorption of vitamin D: from the meal to the enterocyte. *Food & function* **6**, 356-362

23.   Asmussen, N., Lin, Z., McClure, M. J., Schwartz, Z., and Boyan, B. D. (2017) Regulation of extracellular matrix vesicles via rapid responses to steroid hormones during endochondral bone formation. *Steroids*

24.   Tian, X. Q., and Holick, M. F. (1999) A liposomal model that mimics the cutaneous production of vitamin D-3 - Studies of the mechanism of the membrane-enhanced thermal isomerization of previtamin D-3 to vitamin D-3. *J Biol Chem* **274**, 4174-4179

25.   Lisetski, L. N., Gluhova Ya, E., Vashchenko, O. V., and Kasian, N. A. (2012) Effect of the vitamin D photosynthesis products on thermodynamic parameters of model lipid membranes. *Biopolymers and Cell* **28**, 114-120

26.   Raudino, A., Castelli, F., Sarpietro, M. G., and Cambria, A. (1994) CALORIMETRIC ANALYSIS OF LIPID-STEROL SYSTEMS - A COMPARISON BETWEEN STRUCTURALLY SIMILAR CHOLESTEROL AND VITAMIN-D-3 INTERACTING WITH PHOSPHOLIPID-BILAYERS OF DIFFERENT THICKNESS. *Chem Phys Lipids* **74**, 25-37

27.   Kamal, M. A., Pal, A., and Raghunathan, V. A. (2012) Modulated phases of lipid membranes induced by sterol derivatives. *Soft Matter* **8**, 11600-11603

28.   Kazanci, N., Toyran, N., Haris, P. I., and Severcan, F. (2001) Vitamin D2 at high and low concentrations exert opposing effects on molecular order and dynamics of dipalmitoyl phosphatidylcholine membranes. *Spectroscopy* **15**

29. Toyran, N., and Severcan, F. (2002) Infrared Spectroscopic Studies on the Dipalmitoyl Phosphatidylcholine Bilayer Interactions with Calcium Phosphate: Effect of Vitamin D2. *Spectroscopy* **16**

30. Toyran, N., and Severcan, F. (2007) Interaction between vitamin D2 and magnesium in liposomes: Differential scanning calorimetry and FTIR spectroscopy studies. *Journal of Molecular Structure* **839**, 19-27

31. Chaves, M. A., Oseliero, P. L., Jange, C. G., Sinigaglia-Coimbra, R., Oliveira, C. L. P., and Pinho, S. C. (2018) Structural characterization of multilamellar liposomes coencapsulating curcumin and vitamin D-3. *Colloids and Surfaces a-Physicochemical and Engineering Aspects* **549**, 112-121

32. Mendelsohn, R., and Moore, D. J. (1998) Vibrational spectroscopic studies of lipid domains in biomembranes and model systems. *Chem Phys Lipids* **96**, 141-157

33. Lewis, R. N., and McElhaney, R. N. (2013) Membrane lipid phase transitions and phase organization studied by Fourier transform infrared spectroscopy. *Biochim Biophys Acta* **1828**, 2347-2358

34. Zhang, Y. P., Lewis, R. N., and McElhaney, R. N. (1997) Calorimetric and spectroscopic studies of the thermotropic phase behavior of the n-saturated 1,2-diacylphosphatidylglycerols. *Biophys J* **72**, 779-793

35. Ishikawa, S., and Ando, I. (1992) Structural Studies of Dimyristoylphosphatidylcholine and Distearoylphosphatidylcholine in the Crystalline and Liquid-Crystalline States by Variable-Temperature Solid-State High-Resolution C-13 NMR-Spectroscopy. *Journal of Molecular Structure* **271**, 57-73

36. Clarke, J. A., Heron, A. J., Seddon, J. M., and Law, R. V. (2006) The diversity of the liquid ordered (L(o)) phase of phosphatidylcholine/cholesterol membranes: A variable temperature multinuclear solid-state NMR and X-ray diffraction study. *Biophys J* **90**, 2383-2393

37. Guo, W., and Hamilton, J. A. (1995) A MULTINUCLEAR SOLID-STATE NMR-STUDY OF PHOSPHOLIPID-CHOLESTEROL INTERACTIONS - DIPALMITOYLPHOSPHATIDYLCHOLINE-CHOLESTEROL BINARY-SYSTEM. *Biochemistry-Us* **34**, 14174-14184

38. Hubner, W., and Blume, A. (1998) Interactions at the lipid-water interface. *Chem Phys Lipids* **96**, 99-123

39. Hubner, W., and Mantsch, H. H. (1991) ORIENTATION OF SPECIFICALLY C-13=O LABELED PHOSPHATIDYLCHOLINE MULTILAYERS FROM POLARIZED ATTENUATED TOTAL REFLECTION FT-IR SPECTROSCOPY. *Biophys J* **59**, 1261-1272

40. Lewis, R., Pohle, W., and McElhaney, R. N. (1996) The interfacial structure of phospholipid bilayers: Differential scanning calorimetry and Fourier transform infrared spectroscopic studies of 1,2-dipalmitoyl-sn-glycero-3-phosphorylcholine and its dialkyl and acyl-alkyl analogs. *Biophys J* **70**, 2736-2746

41. Nilsson, A., Holmgren, A., and Lindblom, G. (1991) FOURIER-TRANSFORM INFRARED-SPECTROSCOPY STUDY OF DIOLEOYLPHOSPHATIDYLCHOLINE AND MONOOLEOYLGLYCEROL IN LAMELLAR AND CUBIC LIQUID-CRYSTALS. *Biochemistry-Us* **30**, 2126-2133

42. Arrondo, J. L. R., Goni, F. M., and Macarulla, J. M. (1984) INFRARED-SPECTROSCOPY OF PHOSPHATIDYLCHOLINES IN AQUEOUS SUSPENSION - A STUDY OF THE PHOSPHATE GROUP VIBRATIONS. *Biochim Biophys Acta* **794**, 165-168

43. Grdadolnik, J., and Hadzi, D. (1993) CONFORMATIONAL EFFECTS OF METAL SALT BINDING TO THE POLAR HEAD OF PHOSPHATIDYLCHOLINES INVESTIGATED BY FTIR SPECTROSCOPY. *Chem Phys Lipids* **65**, 121-132

44. Iraolagoitia, X. L. R., and Martini, M. F. (2010) Ca2+ adsorption to lipid membranes and the effect of cholesterol in their composition. *Colloid Surface B* **76**, 215-220